EMBO reports

scientific report

Loss of autophagy in hypothalamic POMC neurons impairs lipolysis

Susmita Kaushik[1,2], Esperanza Arias[1,2*], Hyokjoon Kwon[1,3,4], Nuria Martinez Lopez[1,3,4], Diana Athonvarangkul[1,3,4], Srabani Sahu[1,3,4], Gary J. Schwartz[1,2,4,5], Jeffrey E. Pessin[1,2,3,4] & Rajat Singh[1,2,3,4+]*

[1]Department of Medicine, [2]Institute for Aging Research, [3]Department of Molecular Pharmacology, [4]Diabetes Research Center, and [5]Department of Neuroscience, Albert Einstein College of Medicine, Bronx, New York, USA

Autophagy degrades cytoplasmic contents to achieve cellular homeostasis. We show that selective loss of autophagy in hypothalamic proopiomelanocortin (POMC) neurons decreases α-melanocyte-stimulating hormone (MSH) levels, promoting adiposity, impairing lipolysis and altering glucose homeostasis. Ageing reduces hypothalamic autophagy and α-MSH levels, and aged-mice phenocopy, the adiposity and lipolytic defect observed in POMC neuron autophagy-null mice. Intraperitoneal isoproterenol restores lipolysis in both models, demonstrating normal adipocyte catecholamine responsiveness. We propose that an unconventional, autophagosome-mediated form of secretion in POMC neurons controls energy balance by regulating α-MSH production. Modulating hypothalamic autophagy might have implications for preventing obesity and metabolic syndrome of ageing.

Keywords: autophagy; ageing; hypothalamus; obesity; POMC

EMBO *reports* (2012) **13**, 258–265. doi:10.1038/embor.2011.260

INTRODUCTION

Nutritional surplus and reduced energy expenditure promote adiposity and glucose intolerance, the hallmarks of the metabolic syndrome. The hypothalamic agouti-related peptide (AgRP) and proopiomelanocortin (POMC) neurons integrate nutritional and hormonal cues to control energy balance [1]. The AgRP neurons release AgRP that promotes food intake, whereas POMC neurons express POMC preproprotein that is processed to generate adrenocorticotrophic hormone (ACTH) and α-melanocyte-stimulating hormone (MSH) [2]. α-MSH activates central melanocortin receptors to curtail food intake and promote energy expenditure by modulating sympathetic outputs to the periphery [3].

Macroautophagy (hereafter autophagy) maintains cellular homeostasis by sequestering cytosolic cargo within autophagosomes and delivering these to lysosomes for degradation [4]. The ubiquitin E1-like ligase, Atg7 initiates membrane elongation by mediating LC3 (microtubule-associated light chain 3) and Atg5-12 conjugation [4]. A well-known inhibitor of autophagy is the mammalian target of rapamycin (mTOR) [4]. Hypothalamic mTOR regulates food intake [5] suggesting that central mTOR might mediate these effects in part by modulating autophagy. In fact, autophagy in AgRP neurons has been shown to control food intake and energy balance [6]. As autophagy declines with ageing [7] it is plausible that decreased hypothalamic autophagy might contribute to the metabolic dysregulation observed with age. Recent studies in yeast [8–10] and in mammalian systems, including osteoclasts [11] and immune cells [12], have revealed new unconventional roles for autophagy proteins in the secretion of cellular proteins. These findings have led us to explore the possibility of similar autophagosome-dependent mechanisms in the nutrient-sensing hypothalamic neurons that might mediate nutrient-driven peptide processing and secretion. Here, we hypothesize that autophagic components contribute to POMC processing to generate α-MSH, and that reduced autophagy in POMC neurons promotes adiposity in part from decreased α-MSH availability. The hypothesis was tested in POMC neuron-selective *atg7*-deficient mice (knockout (KO)), and during reduced autophagy in normally aged mice.

RESULTS AND DISCUSSION

Loss of *atg7* in POMC neurons promotes adiposity

To test whether autophagy in hypothalamic POMC neurons is required for energy balance, we generated KO mice by crossing $Atg7^{F/F}$ mice with rodents that expressed *cre* in POMC neurons. Selective loss of autophagy in POMC neurons was confirmed by colocalization of cre with POMC (Fig 1A), and by demonstrating the absence of Atg7 (Fig 1B) and accumulation of autophagy substrate p62 in POMC neurons from KO mice (Fig 1C). KO mice did not display increased neuronal apoptosis as determined by TdT-mediated dUTP nick end labelling staining (Fig 1D) or POMC

[1]Department of Medicine,
[2]Institute for Aging Research,
[3]Department of Molecular Pharmacology,
[4]Diabetes Research Center, and
[5]Department of Neuroscience, Albert Einstein College of Medicine, Bronx, New York 10461, USA
*These authors contributed equally to this work
+Corresponding author. Tel: +1 718 430 4118; Fax: +1 718 430 8557;
E-mail: rajat.singh@einstein.yu.edu

Received 20 September 2011; revised 16 December 2011; accepted 16 December 2011; published online 17 January 2012

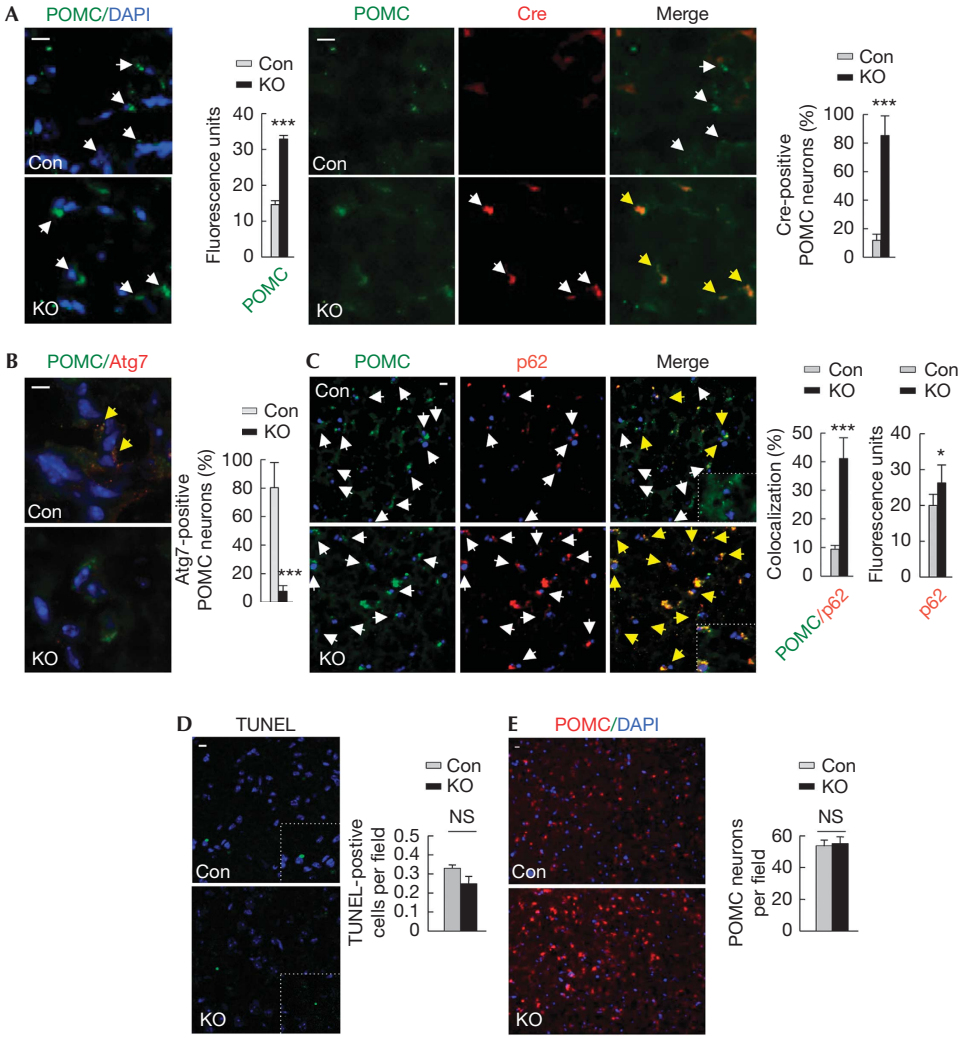

Fig 1 | POMC neuron-selective loss of autophagy. (**A**) Immunofluorescence for POMC (green) and Cre (red; $n=4$), (**B**) POMC (green) and Atg7 (red; $n=4$) and (**C**) POMC (green) and p62 (red; $n=6$) in MBH sections from Con and $Atg7^{F/F}$-POMC-Cre (KO) mice. (**D**) TUNEL-positivity (green; $n=4$) and (**E**) number of POMC-positive neurons (red) in MBH sections from Con and KO mice ($n=6$). Values are mean ± s.e.m. *P* values are as compared with diet- and age-matched controls. $^{*}P<0.05$, $^{***}P<0.001$. Nuclei are blue (DAPI). Scale inset: 10 μm. White arrows indicate Atg7, Cre, p62 or POMC signal. Yellow arrows indicate merged signal. Con, control; DAPI, 4′-6-diamidino-2-phenylindole; KO, knockout; MBH, mediobasal hypothalamic; NS, not statistically significant; POMC, proopiomelanocortin; TUNEL, TdT-mediated dUTP nick end labelling.

neuronal loss (Fig 1E) or increased mortality or neurological deficits (data not shown) when compared with controls. KO mice displayed higher body weights at 2 months (mo; control: 24.7 ± 1.24, KO: 27.5 ± 0.44; $n=9$–13, $P<0.001$) that increased with age (Fig 2A) and upon short-term (2mo) or prolonged (10mo) high-fat diet (HFD) feeding (Fig 2A). Quantitative magnetic resonance spectroscopy (Fig 2B,C) and analyses of epididymal fat (eWAT) weights (Fig 2D,E) revealed that higher body weights of KO mice resulted from increases in body fat and not from changes in lean mass. KO mice displayed increased liver weights (Fig 2F) and triglyceride content (μg/mg tissue weight; control: 19.3 ± 4.6; KO: 35.5 ± 8.3; $n=6$, $P<0.05$) suggesting aberrant hepatic lipid deposition. As POMC-positive cells include pituitary corticotrophs, we asked whether altered corticosterone levels contributed to the adiposity in KO mice. Equivalent plasma corticosterone levels in 4-mo-old control and KO mice (supplementary Fig S1 online) excluded that defective corticotroph function in KO mice contributed to the adiposity.

Autophagy modulates α-MSH levels in POMC neurons

Autophagy in AgRP neurons controls food intake and energy balance by modulating AgRP levels [6], consequently we asked whether loss of autophagy in POMC neurons affected hypothalamic anorexic peptides to promote adiposity. Loss of autophagy in POMC neurons increased hypothalamic levels of POMC preproprotein (Figs 1A,E,2G,I) and its cleavage product ACTH (Fig 2G), without affecting those of neuropeptide Y (Fig 2H) or AgRP (data not shown). Acutely inhibiting autophagy in hypothalamic N41 cells with 3-methyladenine (3MA), verified by decreased LC3-II flux (supplementary Fig S2A online), modestly increased cellular POMC levels (supplementary Fig S2B online). However, addition of methylpyruvate (MP), an exogenous

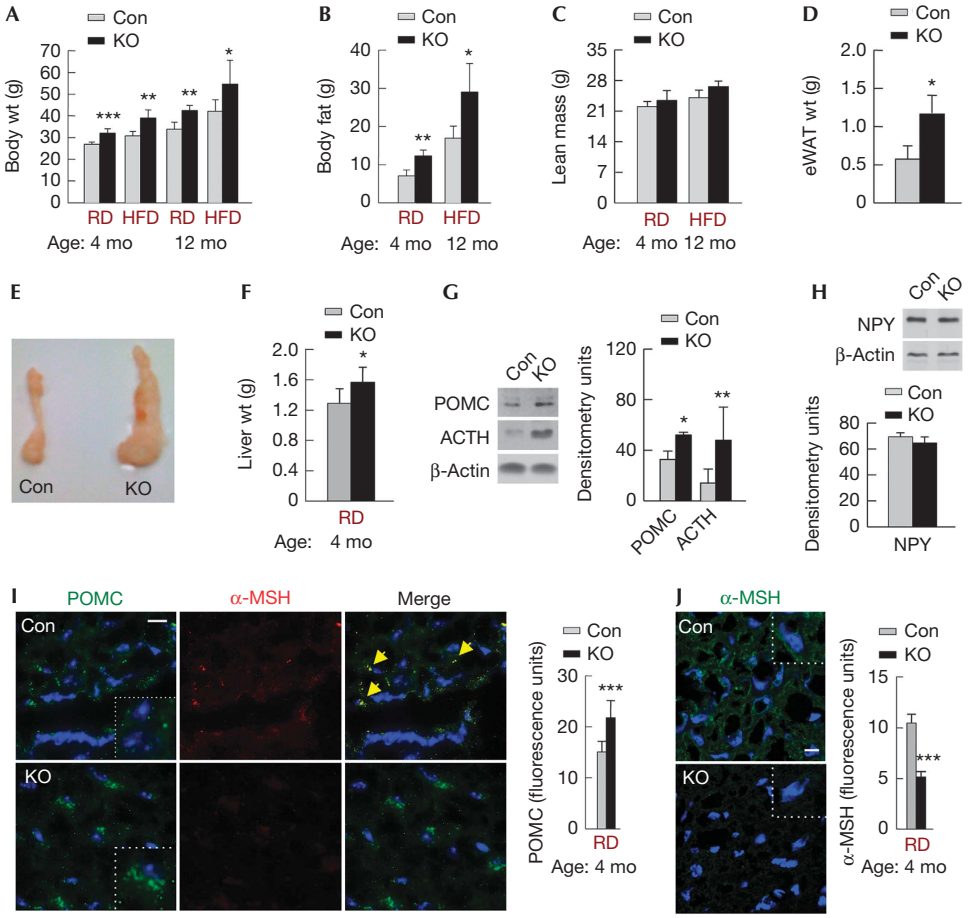

Fig 2 | Loss of *atg7* in POMC neurons promotes adiposity. (**A**) Body wt of 4-mo- and 12-mo-old Con and KO mice on RD ($n = 9–13$) or HFD ($n = 5–7$). (**B**) Total body fat and (**C**) lean mass of 4-mo-old Con and KO mice on RD ($n = 7$) and 12-mo-old Con and KO mice on HFD ($n = 6–8$). (**D**) eWAT wt, (**E**) fat pads and (**F**) liver wt of 4-mo-old Con and KO mice on RD ($n = 6–8$). (**G**) Immunoblots for POMC and ACTH, and (**H**) NPY in MBH from RD-fed Con and KO mice ($n = 3–4$). (**I**) Immunofluorescence for POMC (green) and α-MSH (red), and (**J**) α-MSH (green) in MBH from Con and KO mice on RD ($n = 5$). Values are mean ± s.e.m. *P* values are as compared with diet- and age-matched controls. *$P < 0.05$, **$P < 0.01$, ***$P < 0.001$. Nuclei are blue (DAPI). Scale inset: 10 μm. Yellow arrows indicate merged signal. ACTH, adrenocorticotrophic hormone; Con, control; DAPI, 4′-6-diamidino-2-phenylindole; eWAT, epididymal fat; HDF, high-fat diet; KO, knockout; MBH, mediobasal hypothalamic; mo, month; MSH, melanocyte-stimulating hormone; NPY, neuropeptide Y; POMC, proopiomelanocortin; RD, regular chow; wt, weight.

nutrient, to N41 cells significantly raised levels of both POMC and ACTH in 3MA-treated cells (supplementary Fig S2B,F online; scheme in supplementary Fig S2C online). MP increased cellular c-fos levels indicating the activation of these cells in presence of nutrients (supplementary Fig S2B online). Blocking autophagy by preventing lysosomal degradation with ammonium chloride and leupeptin (inhibitors, Inh), as confirmed by increased p62 accumulation (supplementary Fig S2D online), also increased POMC levels under basal conditions (data not shown) and in response to MP (supplementary Fig S2E online, top) or serum (supplementary Fig S2E online, bottom; scheme in supplementary Fig S2C online). We next asked whether autophagy is required to generate α-MSH, and that hypothalamic accumulation of POMC and ACTH in the absence of autophagy occurred from the failure to generate α-MSH. Indeed, mediobasal hypothalamic (MBH) sections from KO mice displayed markedly reduced immunostaining for α-MSH (Fig 2I,J), which was consistent with increased food intake by these rodents (supplementary Fig S3 online). Inhibiting autophagy in N41 cells (Inh or 3MA) also reduced nutrient (MP)-induced increases of α-MSH levels (supplementary Fig S2G online). Although treatment with rapamycin, which activates autophagy by reducing mTOR phosphorylation (supplementary Fig S2D online), did not modify cellular POMC levels (supplementary Fig S2E online, top and bottom), the activation of autophagy led to localization of α-MSH to cellular projections (supplementary Fig S2G online) supporting our hypothesis that autophagy is required for the generation, and possibly, secretion of α-MSH.

POMC neuronal autophagy is required for lipolysis

As the central melanocortin system regulates peripheral energy expenditure [3], we next asked whether adiposity from loss of autophagy in POMC neurons occurred from impaired peripheral lipid mobilization. To test this we subjected control and KO rodents to quantitative magnetic resonance spectroscopy analyses for body composition before and after a 24 h fast. Although there

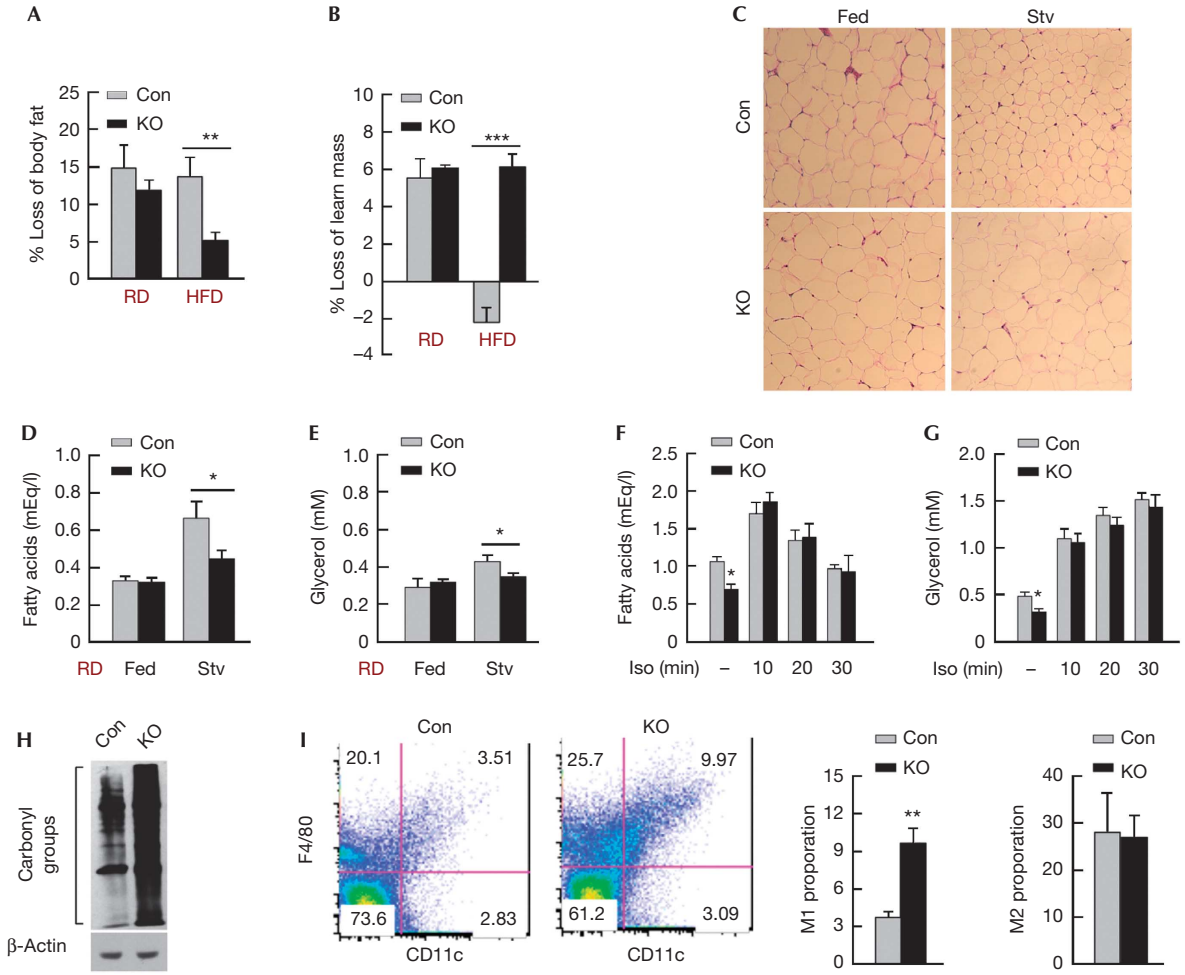

Fig 3 | POMC neuronal autophagy is required for lipolysis. (**A**) Percent loss of body fat and (**B**) lean mass in 24-h-fasted Con and KO mice on RD or HFD ($n = 6$–8). (**C**) Histology for eWAT from fed or 6-h-fasted Con and KO mice on RD ($n = 3$–4). (**D**) Serum fatty acids and (**E**) glycerol from fed or 6-h-fasted Con and KO mice on RD ($n = 7$–9). (**F**) Serum fatty acids and (**G**) glycerol after intraperitoneal isoproterenol (Iso) in 6-h-fasted Con and KO mice on RD ($n = 5$–6). (**H**) Immunoblot for oxidized proteins in eWAT from RD-fed Con and KO mice ($n = 3$). (**I**) FACS analysis for M1 and M2 macrophage proportions in adipose stromal vascular fractions from fed Con and KO mice on RD ($n = 3$). Values are mean ± s.e.m. *P* values are as compared with diet- and age-matched controls. $^*P < 0.05$, $^{**}P < 0.01$, $^{***}P < 0.001$. Con, control; eWAT, epididymal fat; FACS, fluorescence-activated cell sorting; HDF, high-fat diet; Iso, isoproterenol; KO, knockout; POMC, proopiomelanocortin; RD, regular chow; Stv, fasted.

was a trend for fasted KO mice on regular chow (RD) to lose less adipose mass, HFD-fed KO rodents were remarkably resistant to fasting-induced loss of body fat when contrasted to diet-matched controls (Fig 3A). Surprisingly, HFD-fed KO mice significantly decreased their lean mass in response to fasting (Fig 3B), suggesting that KO mice resisted fasting-induced lipolysis, and thus used muscle protein for energy. To test the possibility of defective lipid mobilization in KO mice, eWAT from fed and overnight-fasted control and KO mice were subjected to histological analysis for adipocyte size. Although fasting reduced adipocyte size in controls reflecting mobilization of lipid stores, adipocytes from KO rodents were resistant to reduction in cell size (Fig 3C). To provide functional evidence for defective lipolysis in KO mice, RD- or HFD-fed cohorts were 6 h fasted and analysed for serum-free fatty acid and glycerol levels. As expected, fasted KO rodents on RD or HFD displayed reduced circulating levels of free fatty acids (Fig 3D; supplementary Fig S4A online) and glycerol (Fig 3E; supplementary Fig S4B online) when compared with controls. Decreased lipolysis was restored by intraperitoneal (i.p.) administration of sympathomimetic isoproterenol to KO rodents (Fig 3F,G) suggesting normal adipocyte catecholamine responsiveness, as supported by our findings of equivalent β3-adrenergic receptor messenger RNA levels in eWAT from control and KO mice (supplementary Fig S4C online). These results also suggest that reduced lipolysis might have occurred from diminished central sympathetic tone to the periphery from loss of *atg7* in POMC neurons. Hypothalamic POMC neurons project to neurons in the hindbrain nucleus of the tractus solitarius [13] that, in turn, contribute to neural circuits that supply peripheral tissues [14]. Thus, it is likely that autophagy in hypothalamic POMC neurons singularly or in concert with NTS (nucleus of the tractus solitarius) neurons modulates central sympathetic outputs to the periphery. This conclusion is supported by our observations of reduced expression of *PGC-1α*

(supplementary Fig S4D online) and *UCP-1* (supplementary Fig S4E online) genes in eWAT from KO mice, which typically correlate directly with adipose sympathetic nerve activity [15].

To examine further the peripheral consequences of loss of autophagy in POMC neurons, we subjected eWAT from control and KO rodents to immunoblotting for protein carbonylation reflecting oxidized protein load, and the respective stromal vascular fractions to flow cytometric analyses for the F4/80 + CD11c + pro-inflammatory M1, and F4/80 + CD11c − anti-inflammatory M2 macrophage populations. The KO mice displayed elevated adipose protein oxidation (Fig 3H), and increases in the relative proportion of adipose M1 pro-inflammatory macrophages, without affecting the M2 phenotype (Fig 3I). Surprisingly, increases in the M1 macrophage proportion occurred despite reduced total amount of adipose tissue infiltrated macrophages in the lipolysis-deficient KO mice (supplementary Fig S5A online), as confirmed by decreased adipose expression of macrophage-specific gene *Emr1* (supplementary Fig S5B online). Although these results agree with a recent study showing a role for lipolysis in adipose tissue infiltrated macrophage recruitment, [16] our data showing an approximately threefold increase in the proportion of M1 macrophages in the lipolysis-deficient KO mice, suggest that additional mechanisms might skew adipose macrophages towards the M1 form in a fatty acid-independent manner.

Loss of POMC neuronal *atg7* impairs glucose tolerance

As obesity typically associates with reduced insulin sensitivity, we asked whether adiposity and inflammation in KO mice altered glucose homeostasis. To test this, we first examined basal blood glucose levels in 6-mo- and 12-mo-old RD-fed control and KO mice, and in 12-mo-old cohorts fed a HFD. The loss of autophagy in POMC neurons significantly increased blood glucose levels in mice on RD (Fig 4A,B) or HFD (Fig 4C) when compared with controls. Analyses for serum insulin levels in fed or 6-h-fasted RD-fed cohorts revealed marked elevations in serum insulin levels in KO mice when contrasted to controls (Fig 4D,E) and consequently, homeostasis model of insulin resistance [17] values were elevated in KO mice indicating decreased insulin sensitivity (Fig 4F,G). Glucose tolerance tests revealed significantly reduced glucose clearance in KO mice, regardless of the diet (Fig 4H,I). Insulin tolerance tests showed the inability of KO mice to reduce blood glucose levels in response to exogenous insulin (Fig 4J,K). Altered insulin tolerance tests were also observed in young 1-mo-old KO mice (Fig 4L) with similar body weights as age-matched controls (Fig 4M), suggesting that loss of autophagy in POMC neurons was sufficient to dysregulate glucose homeostasis before onset of adiposity. Although the mechanisms that contribute to glucose intolerance in KO mice need to be examined, our results demonstrate a central role for POMC neuronal autophagy in control of glucose homeostasis.

Ageing reduces POMC neuronal autophagy and lipolysis

As autophagy is considered to decrease with age [7], we asked whether normally aged mice (22mo) are defective for hypothalamic autophagy. Indeed, ageing reduced hypothalamic Atg7 levels (Fig 5A) and decreased steady-state levels of LC3-II, indicating reduced autophagosome content (Fig 5B). Functional autophagy flux assays revealed reduced rate of autophagolysosomal fusion (Fig 5C, left), and decreased lysosomal accumulation of autophagy substrates, LC3-II (Fig 5C, right), p62 (Fig 5D, left), and neighbour of BRCA1 gene 1 (NBR1), the newly elucidated autophagy receptor [18], (Fig 5D, left) in aged hypothalami. Although, ageing did not significantly modify basal p62 and NBR1 levels in total hypothalamic lysates (Fig 5D, right), aged mice revealed marked accumulation of p62 predominantly within POMC neurons (Fig 5E, left and middle), suggesting increased sensitivity of POMC neurons to reduced autophagy with age. In agreement with altered hypothalamic peptide levels in KO mice (Fig 2G,I,J), reduced autophagy during ageing increased hypothalamic POMC preproprotein (Fig 5E right, and F) and ACTH levels (Fig 5F), and reduced those of α-MSH (Fig 5G). In addition, aged rodents phenocopied the adiposity and lipolytic defects observed in KO rodents, as reflected by increased body weight (Fig 5H), adipose expansion (Fig 5I) and reduced fasting-induced serum-free fatty acids (Fig 5J), and glycerol (Fig 5K) when compared with young (3mo) mice. Decreased lipolysis in mice was restored by i.p. isoproterenol (Fig 5L,M), despite reduced adipose triglyceride lipase levels (Fig 5N) demonstrating maintained adipose catecholamine responsiveness during ageing. Restoration of adipose lipolysis upon peripheral sympathetic stimulation in two models of reduced hypothalamic autophagy, that is, during ageing, and following deletion of *atg7*, demonstrates a crucial role for hypothalamic autophagy in maintenance of central sympathetic lipolytic signals to peripheral tissues.

In totality, our results reveal that POMC neuronal autophagy is required for maintenance of energy balance through generation of α-MSH, and that reduced autophagy in POMC neurons might contribute, in part, to the metabolic disturbances observed during ageing. We suggest a possible role for an unconventional form of autophagosome-mediated processing of ACTH into α-MSH (supplementary Fig S6 online). Recent studies have highlighted roles for autophagosomes in secretion of cytosolic proteins as diverse as acyl coenzyme A-binding protein in the yeast [8–10] or the inflammatory cytokine interleukin-1 [12] by a function that occurs independent of its fusion with lysosomes. We propose that autophagy proteins might also modulate the processing, and possibly secretion, of neuronal proteins. Thus, modulating autophagy in POMC neurons for control of whole-body energy balance might have implications for developing new strategies against obesity, and the metabolic syndrome of ageing.

METHODS

Animals and cells. KO mice were generated by crossing $Atg7^{F/F}$ (Drs M. Komatsu and K. Tanaka, Tokyo Metropolitan Institute of Medical Science) with POMC-Cre mice (Jackson Laboratories, Bar Harbor, ME, USA). Aged (22 mo) and young (3 mo) mice were obtained from the NIH National Institute on Aging (Bethesda, MD, USA). Studies were performed in male mice under a protocol approved by the institutional animal care and use committee. Mice were fed RD (5058; Lab Diet, St Louis, MO, USA) or a HFD (60% kcal in fat; D12492; Research Diets, New Brunswick, NJ, USA), and maintained on 12-h light/dark cycles. Fasting was initiated at the beginning of the dark cycle. Genotyping was done with described primers [6]. Mouse hypothalamic N41 cells were grown in high glucose (4.5 g/l), glutamine-supplemented DMEM (Invitrogen, Carlsbad, CA, USA) with 10% fetal bovine serum (Invitrogen) and antibiotics. For experiments, hypothalamic cells were transferred to serum-free DMEM.

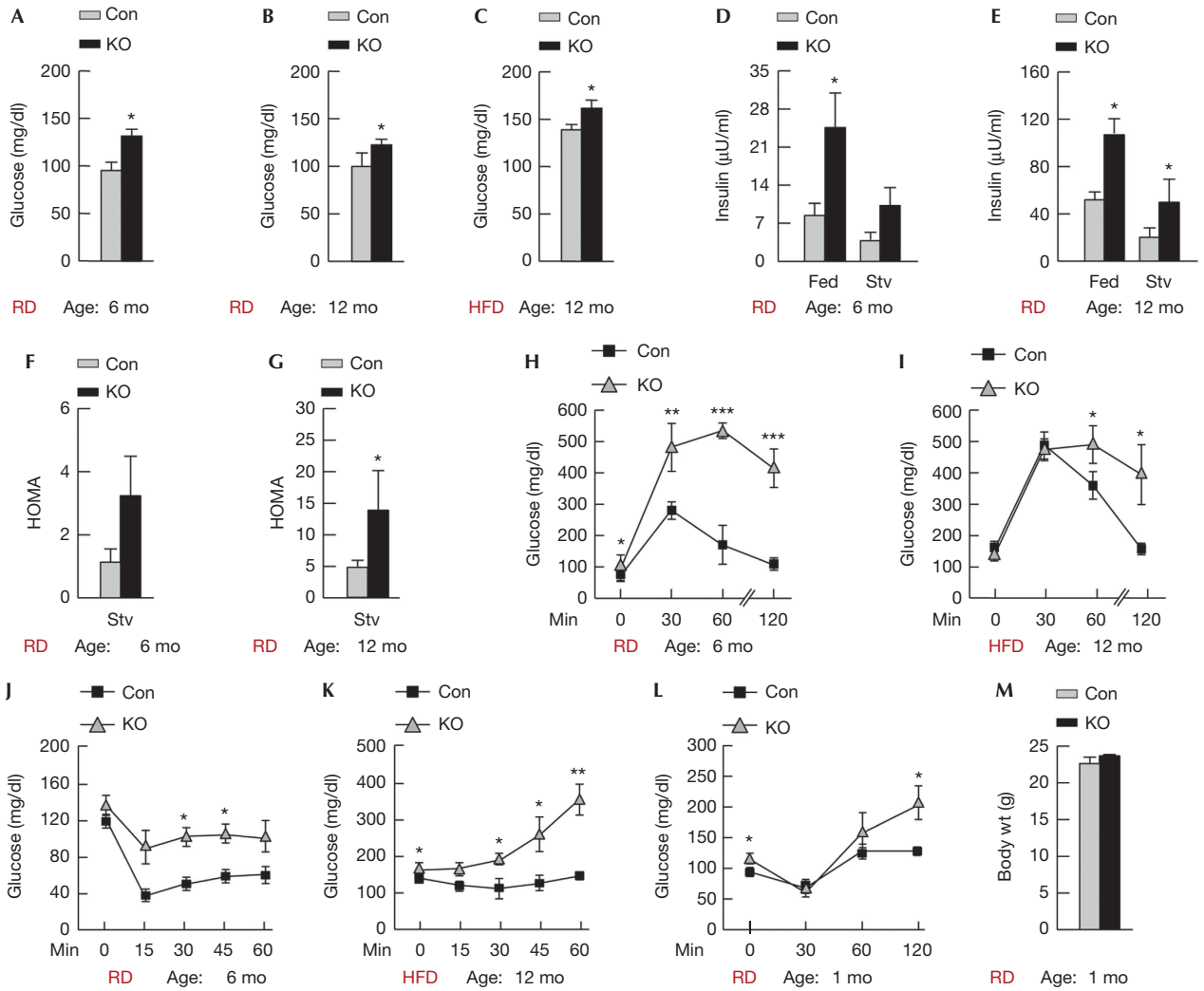

Fig 4 | Loss of POMC neuronal *atg7* impairs glucose tolerance. (**A**) Blood glucose levels in 6 mo ($n = 7$–9) and (**B**) 12 mo Con and KO mice on RD ($n = 6$), and in (**C**) 12-mo-old Con and KO mice on HFD ($n = 4$). (**D**) Serum insulin levels in 6 mo, ($n = 7$–9) and (**E**) 12-mo-old RD-fed Con and KO mice that were fed or 6 h fasted ($n = 6$). (**F**) HOMA values from 6-h-fasted 6-mo-old ($n = 7$–9) and (**G**) 12-mo-old Con and KO mice ($n = 6$) on RD. (**H**) Glucose tolerance tests in 6-h-fasted 6-mo-old mice on RD ($n = 4$) and in (**I**) 6-h-fasted 12-mo-old Con and KO mice fed HFD for 10 mo ($n = 4$). (**J**) Insulin tolerance tests in RD-fed 6-mo-old ($n = 4$) and (**K**) HFD-fed 12-mo-old Con and KO mice ($n = 4$). (**L**) Insulin tolerance tests and (**M**) body weights of 1-mo-old Con and KO mice on RD ($n = 3$–5). Values are mean ± s.e.m. *P* values are as compared with diet- and age-matched controls. $^*P < 0.05$, $^{**}P < 0.01$, $^{***}P < 0.001$. Con, control; HDF, high-fat diet; HOMA, homeostasis model of insulin resistance; KO, knockout; mo, month; POMC, proopiomelanocortin; RD, regular chow; Stv, fasted.

Chemicals and antibodies. Antibodies to Atg7, adipose triglyceride lipase, LC3 and P-mTOR (Ser2448) were from Cell Signaling (Danvers, MA, USA), ACTH and POMC from Novus Biologicals (Littleton, CO, USA), α-MSH from Thermo-Fisher (Waltham, MA, USA), Cre from GenScript (Piscataway, NJ, USA), p62 from Enzo life sciences (Plymouth Meeting, PA, USA), c-fos and neuropeptide Y from Santa Cruz Biotechnology (Santa Cruz, CA, USA), NBR1 from Abnova (Walnut, CA, USA), ubiquitin from Invitrogen, and β-actin from Sigma-Aldrich (St Louis, MO, USA). Antibody selectivity for POMC (Novus Biologicals; NB100-1533), ACTH (Novus Biologicals; NBP1-35271) and α-MSH (Thermo-Fisher; PA1-18012) were based on their abilities to recognize non-overlapping epitopes to prevent nonspecificity. Isoproterenol (10 mg/kg body weight), insulin (0.75 U/kg body weight), leupeptin (100 μM), ammonium chloride (20 mM), 3MA (1.5 mg/ml) and rapamycin (100 nM) were from Sigma-Aldrich, and MP (10 μM) from Fluka (Milwaukee, WI, USA).

***In vivo* p62/LC3/NBR1 flux assays.** Autophagic flux assays determined the net amount of autophagy substrates accumulated in lysosomes in presence of lysosomal Inh, ammonium chloride and leupeptin. Briefly, MBH explants were immediately transferred to glutamine-supplemented, high glucose DMEM in presence or absence of Inh at 37 °C/5% CO_2 for 2 h following which explant lysates were immunoblotted for LC3-II, p62 or NBR1. Functional parameters reflecting autophagy flux were expressed as 'rate of autophagolysosome fusion', determined by

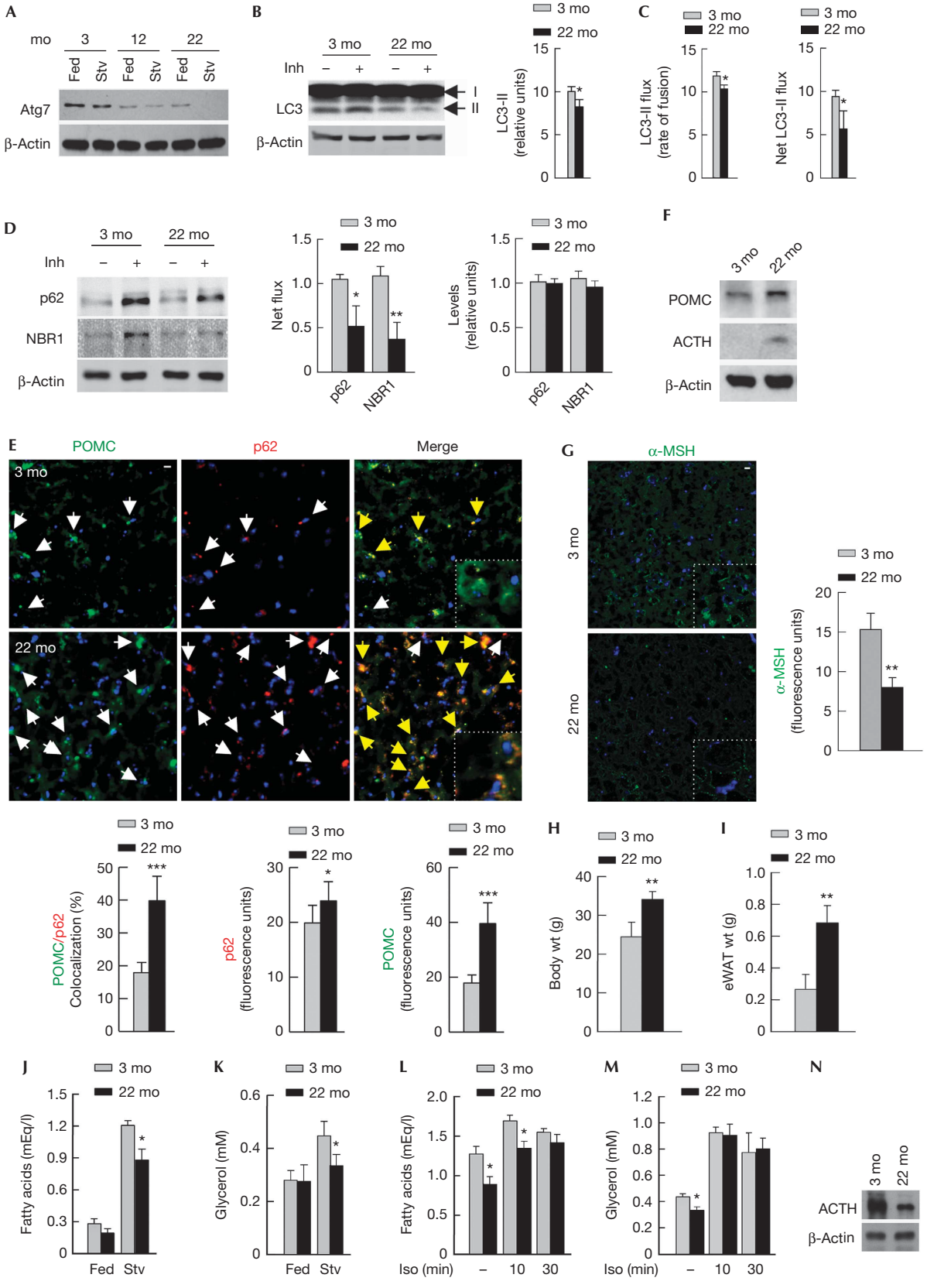

◀ **Fig 5** | Ageing reduces POMC neuronal autophagy and lipolysis. (**A**) Immunoblots for Atg7 in MBH from young (3 mo), middle-aged (12 mo) and aged (22 mo) fed and 6-h-fasted (Stv) mice ($n=4$), and (**B**) LC3-II in MBH explants from 3 mo and 22 mo fed mice in presence or absence of lysosomal inhibitors (Inh) ($n=11$–13). Mean ± s.e.m values for (**B**) steady-state LC3-II and (**C**) LC3-II flux are shown ($n=11$–13). (**D**) Immunoblots for p62 and NBR1 flux in MBH from 3 mo and 22 mo fed mice in presence or absence of Inh ($n=11$–13). (**E**) Immunofluorescence for POMC (green) and p62 (red) ($n=4$), (**F**) immunoblots for POMC and ACTH ($n=4$), and (**G**) immunofluorescence for α-MSH in MBH from 3 mo and 22 mo mice on RD ($n=4$). (**H**) Body wt and (**I**) eWAT wt of 3-mo- and 22-mo-old mice on RD ($n=9$–13). (**J**) Serum fatty acids and (**K**) glycerol from fed or 6-h-fasted (Stv) 3 mo and 22 mo mice ($n=7$–9), and (**L,M**) after intraperitoneal Iso in 6-h-fasted 3 mo and 22 mo mice ($n=5$–6). (**N**) Immunoblots for adipose triglyceride lipase (ATGL) in eWAT from 3 mo and 22 mo mice. Values are mean ± s.e.m. *P* values are as compared with controls. $^{*}P<0.05$, $^{**}P<0.01$, $^{***}P<0.001$. Nuclei are blue (DAPI). Scale inset: 10 μm. Yellow arrows indicate merged signal. ACTH, adrenocorticotrophic hormone; Con, control; eWAT, epididymal fat; Iso, isoproterenol; MBH, mediobasal hypothalamic; mo, months; MSH, melanocyte-stimulating hormone; POMC, proopiomelanocortin; RD, regular chow; wt, weight.

dividing the densitometric value of Inh+ LC3-II by Inh− LC3-II value for the corresponding sample, and as 'net flux' calculated by subtracting the densitometric value of Inh– LC3-II, p62, and NBR1 from those of corresponding Inh+ values.

Immunohistochemistry. MBH sections were prefixed in paraformaldehyde and incubated in 20% sucrose at 4 °C. Sections were acetone fixed at −20 °C, blocked with 3% fetal bovine serum containing 0.01% Triton X-100, treated with primary and fluorophore-tagged secondary antibody (Invitrogen), mounted in 4′-6-diamidino-2-phenylindole (Invitrogen) and observed on an Axiovert 200 (Zeiss, Germany) or a Confocal SP5 AOBS microscope (Leica, Germany). POMC neuron count was estimated in 10 fields per section, 4 sections from each mouse, from 6 control and KO mice, and expressed as number of POMC-positive cells per field. MBH TdT-mediated dUTP nick end labelling staining was done by a commercial kit (Promega, Madison, WI, USA), and observed on a Leica SP5 microscope.

Real-time PCR. Adipose gene expression was determined using SYBR Green in a Smart Cycler II thermocycler (Cepheid, Sunnyvale, CA, USA) as described [6]. Expression of genes for PGC-1α, UCP-1 and β3-adrenergic receptor were normalized to actin. The following primers were used: *pgc-1α* (forward (f)) 5′-CCCTGCCATTGTTAAGACC-3′, (reverse (r)) 5′-TGCTGCTGTTCCTGTTTTC-3′; *ucp-1* (f) 5′-ACTGCCACACCTCCAGTCATT-3′, (r) 5′-CTTTGCCTCACTCAGGATTGG-3′; *Adrβ3* (f) 5′-GGCAACCTGCTGGTAATCAT-3′, (r) 5′-TCCACTGACGTCCACAGTTC-3′.

Statistics. Values are mean + s.e.m, and groups were compared by two-tailed Student's *t*-test using Sigma Plot (Jandel Scientific, San Rafael, CA, USA).

Supplementary information is available at EMBO *reports* online (http://www.emboreports.org).

ACKNOWLEDGEMENTS

This work was supported by the NIH NIDDK grant DK087776 to R.S., and an Einstein-Nathan Shock Center of Excellence in the Basic Biology of Aging pilot grant to R.S., DK033823 to J.E.P., and grants from Skirball Institute for Nutrient Sensing, NY Obesity Research Center DK026687 and Einstein Diabetes Research Center DK020541. S.K. and E.A. are supported by NIH grant T32AG023475, and Micinn/Fulbright Fellowship 2008-0128, respectively.

Author contributions: S.K. and E.A. performed *in vivo* studies and immunohistochemistry on brain sections. H.K. performed fluorescence-activated cell sorting and reverse transcription PCR analyses. NML and D.A. performed immunofluorescence on cells. S.S. assisted in *in vivo* studies. G.J.S. and J.E.P. contributed to data analysis. R.S. conceived the study, analysed data and wrote the paper.

CONFLICT OF INTEREST

The authors declare that they have no conflict of interest.

REFERENCES

1. Belgardt BF, Bruning JC (2010) CNS leptin and insulin action in the control of energy homeostasis. *Ann N Y Acad Sci* **1212:** 97–113
2. D'Agostino G, Diano S (2010) Alpha-melanocyte stimulating hormone: production and degradation. *J Mol Med* **88:** 1195–1201
3. Nogueiras R *et al* (2007) The central melanocortin system directly controls peripheral lipid metabolism. *J Clin Invest* **117:** 3475–3488
4. Singh R, Cuervo AM (2011) Autophagy in the cellular energetic balance. *Cell Metab* **13:** 495–504
5. Cota D, Proulx K, Smith KA, Kozma SC, Thomas G, Woods SC, Seeley RJ (2006) Hypothalamic mTOR signaling regulates food intake. *Science* **312:** 927–930
6. Kaushik S, Rodriguez-Navarro JA, Arias E, Kiffin R, Sahu S, Schwartz GJ, Cuervo AM, Singh R (2011) Autophagy in hypothalamic AgRP neurons regulates food intake and energy balance. *Cell Metab* **14:** 173–183
7. Cuervo AM (2008) Autophagy and aging: keeping that old broom working. *Trends Genet* **24:** 604–612
8. Duran JM, Anjard C, Stefan C, Loomis WF, Malhotra V (2010) Unconventional secretion of Acb1 is mediated by autophagosomes. *J Cell Biol* **188:** 527–536
9. Bruns C, McCaffery JM, Curwin AJ, Duran JM, Malhotra V (2011) Biogenesis of a novel compartment for autophagosome-mediated unconventional protein secretion. *J Cell Biol* **195:** 979–992
10. Manjithaya R, Anjard C, Loomis WF, Subramani S (2010) Unconventional secretion of Pichia pastoris Acb1 is dependent on GRASP protein, peroxisomal functions, and autophagosome formation. *J Cell Biol* **188:** 537–546
11. Deselm CJ *et al* (2011) Autophagy proteins regulate the secretory component of osteoclastic bone resorption. *Dev Cell* **21:** 966–974
12. Dupont N, Jiang S, Pilli M, Ornatowski W, Bhattacharya D, Deretic V (2011) Autophagy-based unconventional secretory pathway for extracellular delivery of IL-1beta. *EMBO J* **30:** 4701–4711
13. Zheng H, Patterson LM, Rhodes CJ, Louis GW, Skibicka KP, Grill HJ, Myers MG Jr, Berthoud HR (2010) A potential role for hypothalamomedullary POMC projections in leptin-induced suppression of food intake. *Am J Physiol Regul Integr Comp Physiol* **298:** R720–R728
14. Stanley S, Pinto S, Segal J, Perez CA, Viale A, DeFalco J, Cai X, Heisler LK, Friedman JM (2010) Identification of neuronal subpopulations that project from hypothalamus to both liver and adipose tissue polysynaptically. *Proc Natl Acad Sci USA* **107:** 7024–7029
15. Ramadori G *et al* (2010) SIRT1 deacetylase in POMC neurons is required for homeostatic defenses against diet-induced obesity. *Cell Metab* **12:** 78–87
16. Kosteli A, Sugaru E, Haemmerle G, Martin JF, Lei J, Zechner R, Ferrante AW Jr (2010) Weight loss and lipolysis promote a dynamic immune response in murine adipose tissue. *J Clin Invest* **120:** 3466–3479
17. Matthews DR, Hosker JP, Rudenski AS, Naylor BA, Treacher DF, Turner RC (1985) Homeostasis model assessment: insulin resistance and β-cell function from fasting plasma glucose and insulin concentrations in man. *Diabetologia* **28:** 412–419
18. Kirkin V *et al* (2009) A role for NBR1 in autophagosomal degradation of ubiquitinated substrates. *Mol Cell* **33:** 505–516